

## Is hexagonal flow $v_6$ just a superposition of elliptic $v_2$ and triangular $v_3$ flows?

E. Zabrodin<sup>1,2,a</sup>, L. Bravina<sup>1</sup>, B.H. Bruchheim Johansson<sup>1,3</sup>, G.Kh. Eyyubova<sup>2,4</sup>, V.L. Korotkikh<sup>2</sup>, I.P. Lokhtin<sup>2</sup>, L.V. Malinina<sup>2,5</sup>, S.V. Petrushanko<sup>2</sup>, and A.M. Snigirev<sup>2</sup>

<sup>1</sup>Department of Physics, University of Oslo, PB 1048 Blindern, Oslo, Norway

<sup>2</sup>Skobeltsyn Institute of Nuclear Physics, Moscow State University, RU-119991 Moscow, Russia

<sup>3</sup>Oslo and Akershus University College of Applied Sciences (HIOA), Oslo, Norway

<sup>4</sup>Czech Technical University in Prague, FNSPE, Prague, Czech Republic

<sup>5</sup>Joint Institute for Nuclear Researches, Dubna, Russia

**Abstract.** HYDJET++ model, which combines parametrized hydrodynamics with jets, is employed to study the dependence of the hexagonal flow,  $v_6$ , on the elliptic,  $v_2$ , and triangular,  $v_3$ , flows. Calculations are performed for lead-lead collisions at  $\sqrt{s} = 2.76$  ATeV with centrality  $10\% \leq \sigma/\sigma_{geo} \leq 50\%$ . Hexagonal flow in the model emerges only due to the presence of  $v_2$  and  $v_3$ . Position of its event plane,  $\Psi_6$ , is found to be closer to  $\Psi_3$  for semi-central events, whereas in peripheral reactions it is closer to  $\Psi_2$ , in line with the experimental analysis of the plane correlations. The amplitude of “induced” hexagonal flow is also comparable with that obtained in experiments. It means, in particular, that many features of the  $v_6$  can be explained by interplay of elliptic and triangular flows.

### 1 Introduction

The collective flow of hadrons as a signal of early stage of hot and dense matter, produced in relativistic heavy-ion collisions, was proposed about 40 years ago [1]. At the beginning, the flow was decomposed into the in-plane bounce-off flow and the squeeze-out flow, elongated perpendicular to the reaction plane. The new method, proposed for the flow analysis in [2, 3], relies on the Fourier decomposition of hadron distribution in the azimuthal plane

$$E \frac{d^3N}{d^3p} = \frac{1}{2\pi} \frac{d^2N}{p_T dp_T dy} \left\{ 1 + 2 \sum_{n=1}^{\infty} v_n \cos [n(\phi - \Psi_n)] \right\}. \quad (1)$$

Here  $p_T$  is the transverse momentum of a particle,  $y$  is the rapidity,  $\phi$  denotes the azimuthal angle between the  $p_T$ , and the participant event plane, while  $v_n$  and  $\Psi_n$  represent the  $n$ -th flow harmonic coefficient and the azimuth of its plane, respectively. The flow harmonics are

$$v_n = \langle \cos [(n(\phi - \Psi_n))] \rangle, \quad (2)$$

---

<sup>a</sup>e-mail: eugen.zabrodin@fys.uio.no

where averaging is taken over all events and all particles in each event. The first three harmonics, called directed  $v_1$ , elliptic  $v_2$ , and triangular  $v_3$  flow, are belonging to lower harmonics, whereas others, such as quadrangular  $v_4$ , pentagonal  $v_5$ , hexagonal  $v_6$  etc. flow, are regarded as higher harmonics.

The studies of heavy-ion collisions within the 2+1 or 3+1 hydrodynamic models are focused particularly on the response of partonic matter to initial density fluctuations. The present status of the investigation of connection between the final flow harmonics  $v_n$  and the initial eccentricities  $\varepsilon_n$  is as follows. Elliptic and triangular flows depend linearly [4] on ellipticity and triangularity, respectively, whereas for higher harmonics this dependence is nonlinear [5].

The aim of our work is to study the partial contributions of lower harmonics to the higher ones. Since the study is performed in the midrapidity range, where the directed flow is very weak compared to the elliptic and triangular flows [6], we will drop  $v_1$  from our consideration and concentrate mainly on the  $v_2$ ,  $v_3$ , and their interplay. The possible connection between lower and higher harmonics was discussed first in [7]. It was shown that in ideal hydrodynamics the quadrangular flow should depend on the elliptic one as  $v_4 = 0.5 v_2^2$  in the limit of large transverse momenta and unique reaction plane  $\Psi$ . Later on every  $n$ -th harmonic was found to possess its own reaction plane  $\Psi_n$ . However, even in the  $\Psi_2$  plane the measured signal  $v_4/v_2^2$  well exceeds the value 0.5, mainly because of its determination not on event-by-event basis [8]. Jets and decays of resonances also increase the ratio [9, 10].

But quadrangular flow gets the major contribution just from one lower harmonic,  $v_2$ . Hexagonal flow is of special interest for us, because it receives the independent contributions from the elliptic and the triangular flows, and has no term proportional to their product,  $v_2 v_3$ . In case of the unique reaction plane and at high transverse momenta the expression for  $v_6$  reads [11]:

$$v_6 \cong \frac{1}{6} v_2^3 + \frac{1}{2} v_3^2. \quad (3)$$

Therefore, it would be interesting to study hexagonal flow, emerging as a result of the interplay of  $v_2$  and  $v_3$ , in case of absence of genuine hexagonal eccentricity  $\varepsilon_6$ , and compare the obtained results with the available experimental data. Jets and decays of resonances can also modify the final distributions. - For instance, the violation of the number-of-constituent-quark (NCQ) scaling at LHC can be explained by the influence of jets, whereas resonances are trying to restore the scaling [9, 10]. - The present study is performed within the HYDJET++ model, which couples parametrized ideal hydrodynamics with jets traversing hot and dense medium. Basic features of the model are given in Sec. 2.

## 2 Elliptic and triangular flows in the HYDJET++ model

The description of the event generator HYDJET++ (HYDroynamics with JETs) can be found elsewhere [12–14]. Recall briefly, that parametrized hydrodynamics is employed [13] to generate soft part of particle spectra, including hadron yields, femtoscopy correlations and differential elliptic flow. In the hard sector the model accounts for radiative and collisional losses [14] for partons traversing hot and dense nuclear matter. Cold nuclear matter effects, such as gluon shadowing [15], are also implemented. Recently [16] the HYDJET++ was modified to generate also the triangular flow,  $v_3$ . Compared to the former transverse radius of the fireball, which reproduces the elliptic deformation

$$R_{ell}(b, \phi) = R_{f0}(b) \frac{\sqrt{1 - \varepsilon^2(b)}}{\sqrt{1 + \varepsilon(b) \cos 2\phi}}, \quad (4)$$

the altered radius of the freeze-out hypersurface in azimuthal plane takes into account triangular deformations as well

$$R(b, \phi) = R_{ell}(b, \phi) \{1 + \varepsilon_3(b) \cos [3(\phi - \Psi_3)]\}. \quad (5)$$

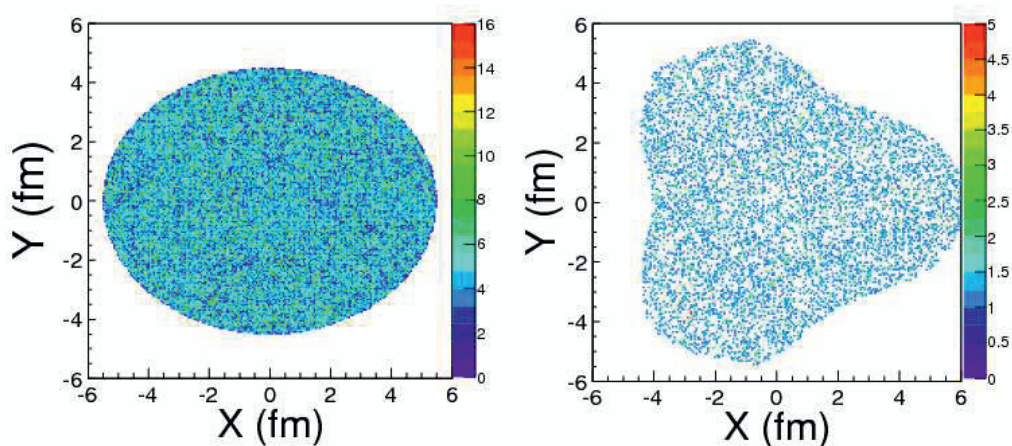


**Figure 1.** A snapshot of the particle density in the azimuthal plane illustrating the generation of second (left plot) and second plus third (right plot) flow harmonics in semiperipheral Pb+Pb collisions generated in HYDJET++ at  $\sqrt{s} = 2.76$  ATeV.

Here  $b$  is the impact parameter and  $R_{f_0}(0)$  is the model parameter which determines the scale of the fireball transverse size at freeze-out. Parameters  $\epsilon(b)$  and  $\epsilon_3(b)$  are responsible for the elliptic and triangular spatial anisotropies, respectively. The event plane of the triangular flow,  $\Psi_3$ , is randomly oriented with respect to the plane  $\Psi_2$ . This means that the generated elliptic and triangular flows are not correlated, in accordance with the experimental observations. The free parameters of the model were tuned to reproduce differential distributions  $v_2(p_T)$  and  $v_3(p_T)$  in Pb+Pb collisions at LHC within the centrality range  $5\% \leq \sigma/\sigma_{geo} \leq 50\%$ . The flow fluctuations in the HYDJET++ arise due to particle momentum distributions and fluctuations of particle multiplicity, which are significantly amplified by the decays of resonances and production of minijets. Figure 1 illustrates generation of the second and the third flow harmonics in HYDJET++ by representing particle densities in the transverse plane. Note that the triangular deformation shown here is very strong. The actual deformations needed to describe triangular flow at LHC energies are typically order of magnitude weaker.

Higher flow harmonics are not explicitly generated in the model, therefore, these harmonics are absent if both  $v_2$  and  $v_3$  is zero. If just the elliptic flow is present, then only even higher harmonics are excited as overtones of the  $v_2$ . Thus, the HYDJET++ provides us a tool to study the pure contributions of both lower harmonics to the higher ones.

### 3 Results for hexagonal flow

Results presented in the Section are based on our two recent studies [11, 16]. About  $2 \cdot 10^6$  Pb+Pb collisions at  $\sqrt{s} = 2.76$  ATeV were generated for each of four centrality bins,  $\sigma/\sigma_{geo} =$

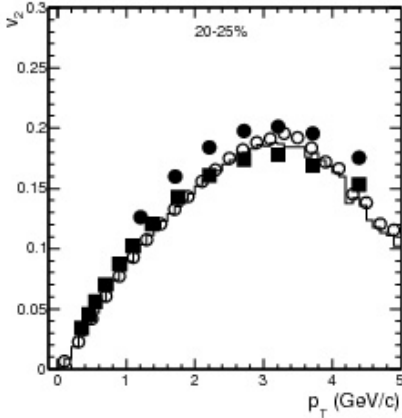


**Figure 2.** Elliptic flow  $v_2(p_T)$  of charged hadrons at pseudo-rapidity  $|\eta| < 0.8$  in Pb+Pb collisions at  $\sqrt{s} = 2.76$  ATeV with centrality 20-25%. Solid circles and solid squares are  $v_2\{2\}$  and  $v_2\{LYZ\}$  from CMS [17], open circles and histogram are  $v_2\{EP\}$  and  $v_2\{\Psi_2\}$  for HYDJET++ events, respectively.

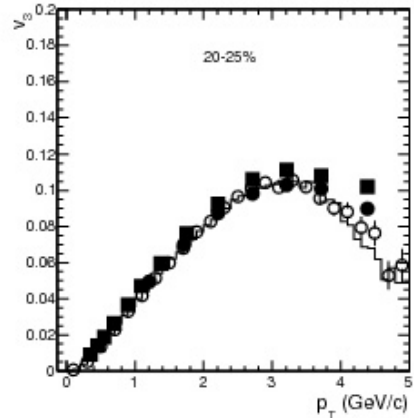


**Figure 3.** The same as Fig.2 but for the triangular flow  $v_3(p_T)$ . Solid circles and solid squares are  $v_3\{2\}$  and  $v_3\{EP\}$  from CMS [18], open circles and histogram are  $v_3\{EP\}$  and  $v_2\{\Psi_3\}$  for HYDJET++ events, respectively.

10 – 20%, 20 – 30%, 30 – 40%, and 40 – 50%. Comparison of the model results with the CMS data at  $20\% \leq \sigma/\sigma_{geo} \leq 25\%$  is given in Figs. 2 and 3 for the elliptic and triangular flows, respectively. The agreement is good. A detailed comparison of the generated flow harmonics from second to sixth with ATLAS and CMS results at different centralities can be found in [16]. Then, the ratio  $v_n^{1/n}/v_2^{1/2}$  is often used to find the possible scaling trends in the behavior of different flow harmonics. Figure 4 presents the ratio  $v_6^{1/6}(p_T)/v_2^{1/2}(p_T)$  in the  $\Psi_2$  plane for charged hadrons produced (a) only in the hydrodynamic part of the calculations and (b) in both soft and hard processes. Recall that hexagonal flow is determined here with respect to the  $\Psi_2$  plane. The horizontal lines show the ideal limit  $v_6^{1/6}/v_2^{1/2} = (1/6)^{1/6} \approx 0.74$ . It is worth mentioning that this limit is attained in pure hydro branch of the calculations already at  $p_T \approx 1$  GeV/c. All four curves are on top of each other. Jets [see Fig. 4(b)] modify this picture by (i) increasing the ratio a bit less than 10% and (ii) causing the rise of its high- $p_T$  tail at  $p_T \geq 3$  GeV/c. Still, there is a hair-width difference between the curves representing the selected centralities.

Similar ratio but for the triangular flow,  $v_6^{1/6}(p_T)/v_3^{1/3}(p_T)$ , in the  $\Psi_3$  plane is displayed in Fig. 5. Here one can see the hierarchy of centralities, i.e., the ratio is larger for more central events. All curves are below the ideal limit  $v_6^{1/6}/v_3^{1/3} = (1/2)^{1/3} \approx 0.89$ , although they seem to approach it with rising  $p_T$ . Jets increase the ratio and make its rise steeper, but no distinct rise of high- $p_T$  tail is observed. Definitely, the partial contributions of elliptic and triangular flows to the hexagonal one should change with centrality.

To verify this hypothesis we plot in Fig. 6  $v_2\{\Psi_2\}$  and  $v_3\{\Psi_3\}$  integrated over transverse momentum within the centrality intervals. The difference between the distributions is obvious. For semicentral collisions  $v_6\{\Psi_2\}$  is weak because the elliptic flow is weak also. Hexagonal flow in  $\Psi_2$  plane becomes stronger with increasing peripherality of collisions. And vice versa,  $v_6\{\Psi_3\}$  is the strongest in semicentral collisions and then gradually drops, despite the slight increase of the triangular flow as the reaction becomes more peripheral.

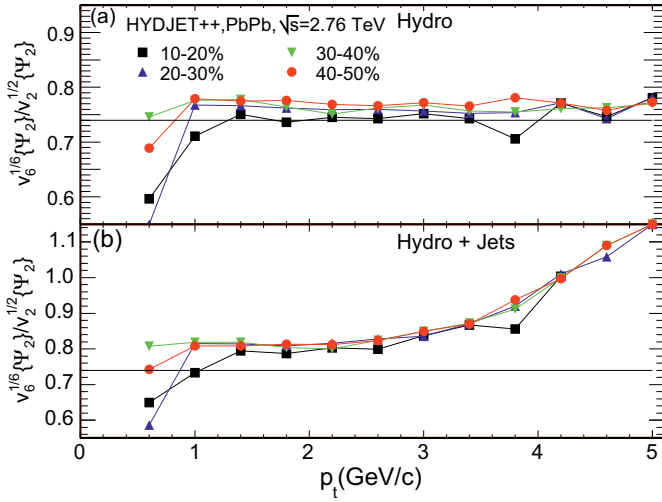


**Figure 4.** Ratio  $v_6^{1/6}/v_2^{1/2}$  as a function of  $p_T$  in the  $\Psi_2$  event plane for charged particles, originated from (a) soft processes only and (b) both soft and hard processes, in HYDJET++ simulations of Pb+Pb collisions at  $\sqrt{s} = 2.76$  ATeV. See text for details.

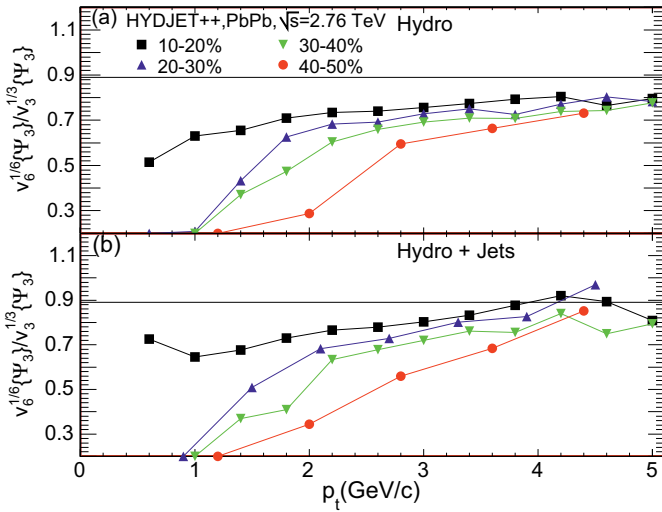


**Figure 5.** The same as Fig.4 but for ratio  $v_6^{1/6}/v_3^{1/3}$  vs.  $p_T$  in the  $\Psi_3$  event plane.

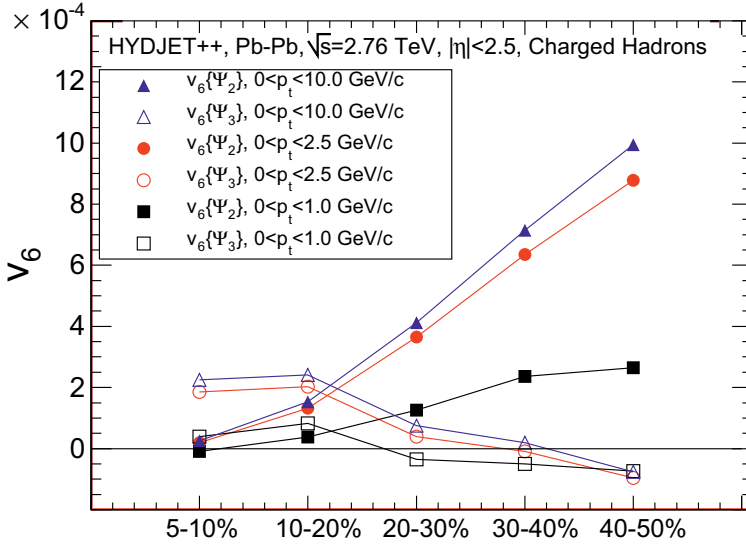


**Figure 6.** Integrated flow  $v_6\{\Psi_2\}$  and  $v_6\{\Psi_3\}$  of charged particles vs. centrality in generated Pb+Pb collisions at  $\sqrt{s} = 2.76$  ATeV.

If so, the same tendency should be revealed in the behavior of the correlators between the event planes. Here the event flow vector  $\vec{Q}_n$  and the event plane angle  $\Psi_n$  should be determined for the flow harmonic of  $n$ -th order [3]

$$\vec{Q}_n = (Q_{n,x}, Q_{n,y}) = \left( \sum_i w_i \cos(n\phi_i), \sum_i w_i \sin(n\phi_i) \right), \quad (6)$$

$$\tan(n\Psi_n) = \frac{Q_{n,y}}{Q_{n,x}}, \quad (7)$$

where  $w_i$  and  $\phi_i$  are the weight and the azimuthal angle of  $i$ -th particle in the lab-system, respectively.

The correlators between arbitrary  $l$  event planes of order  $k_l$  have the form [20–22]  $\langle \cos(\sum_{k=k_{l_{\min}}}^{k_{l_{\max}}} kc_k \Psi_k) \rangle$

with the constraint  $\sum_{k=k_{l_{\min}}}^{k_{l_{\max}}} kc_k = 0$ . For the correlations between  $\Psi_6$  and  $\Psi_2$  (or  $\Psi_3$ ) the corresponding correlators are simply  $\langle \cos 6(\Psi_2 - \Psi_6) \rangle$  and  $\langle \cos 6(\Psi_3 - \Psi_6) \rangle$ . To see the correlations more distinctly we artificially increased the triangular deformation of the freeze-out hypersurface. Both correlators are obtained from the generated events by the method proposed for the analysis of experimental data in [21]. Figure 7 demonstrates that the correlator  $\langle \cos 6(\Psi_2 - \Psi_6) \rangle$  increases for more peripheral collisions. In contrast, the correlator  $\langle \cos 6(\Psi_3 - \Psi_6) \rangle$  drops with rise of the impact parameter, as shown in Fig. 8. These results qualitatively agree with the experimental data [21]. Our explanation is as follows. For the central and semicentral collisions triangular flow is stronger than the elliptic flow, therefore, its contribution to  $v_6$  dominates over the contribution of  $v_2$ . Therefore, the event plane  $\Psi_6$  is closer to

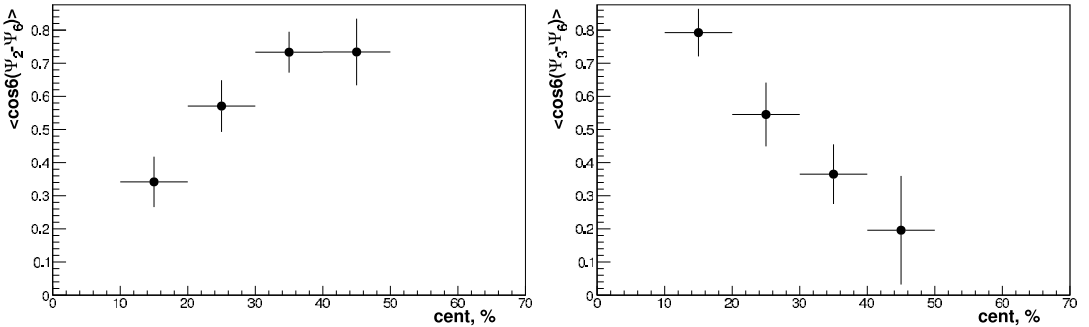


**Figure 7.** Two-plane correlator  $\langle \cos 6(\Psi_2 - \Psi_6) \rangle$  for **Figure 8**. The same as Fig. 7 but for two-plane correlator  $\langle \cos 6(\Psi_3 - \Psi_6) \rangle$  for charged hadrons in generated Pb+Pb collisions at  $\sqrt{s} = 2.76$  ATeV.

the  $\Psi_3$  plane. With the increase of peripherality the elliptic flow becomes significantly stronger, while the triangular flow just slightly increases. Thus, the hexagonal flow is mainly determined by the  $v_2$  for the peripheral collisions. Because  $v_3$  is randomly oriented with respect to  $v_2$ , the correlations between the  $\Psi_6$  plane and the  $\Psi_3$  plane become weaker.

## 4 Conclusions

Our aim was to study the influence of the elliptic and triangular flows on higher harmonics in ultra-relativistic heavy-ion collisions at LHC energies. Hexagonal flow was chosen because it is getting independent contributions from the both lower harmonics,  $v_6 \sim v_2^3 + v_3^2$ . For the ratio  $v_6^{1/6}(p_T)/v_2^{1/2}(p_T)$  in the  $\Psi_2$  plane scaling was found for centralities  $10\% \leq \sigma/\sigma_{geo} \leq 50\%$ . Jets cause the rise of this ratio at  $p_T \geq 3$  GeV/c. Similar effect for Pb+Pb collisions at LHC was observed earlier for the ratio  $v_4(p_T)/v_2^2(p_T)$ .

The analysis of the strength of  $v_6$  as a function of centrality in  $\Psi_2$  and  $\Psi_3$  planes, accomplished by the analysis of the plane correlators  $\langle \cos 6(\Psi_2 - \Psi_6) \rangle$  and  $\langle \cos 6(\Psi_3 - \Psi_6) \rangle$ , shows that hexagonal flow is strongly correlated with  $v_3$  in semicentral events, whereas in semiperipheral and peripheral collisions prevail correlations with  $v_2$ . These findings agree well with the experimental data. Thus, the nonlinear response of the hexagonal flow to the corresponding eccentricity, found in hydrodynamic models, can be explained by the strong influence of the elliptic and the triangular flows and their nonlinear interplay. Further investigations are needed to shed light on this very exciting problem.

## Acknowledgements

*We would like to express our gratitude to the Organisers of the Conference and OAC for the possibility of presenting our results, nice scientific atmosphere, and warm and kind hospitality. This work was supported in parts by the Department of Physics, UiO, Russian Foundation for Basic Research under Grant No. 12-02-91505, a Grant of the President of Russian Federation for Scientific Schools Supporting No. 3920.2012.2, Ministry of Education and Sciences of Russian Federation under agreement No. 8412 and European Union and the Government of Czech Republic under the project "Support for research teams on CTU" No. CZ.1.07/2.3.00/30.0034.*

## References

- [1] W. Scheid, H. Müller, and W. Greiner, *Phys. Rev. Lett.* **32**, 741 (1974)
- [2] S. A. Voloshin and Y. Zhang, *Z. Phys. C* **70**, 665 (1996)
- [3] A. M. Poskanzer and S. A. Voloshin, *Phys. Rev. C* **58**, 1671 (1998)
- [4] G.-Y. Qin, H. Petersen, S. A. Bass, and B. Müller, *Phys. Rev. C* **82**, 064903 (2010)
- [5] U. Heinz and R. Snellings, *Annu. Rev. Nucl. Part. Sci.* **64**, 123 (2013)
- [6] B. Abelev *et al.* (ALICE Collab.), *Phys. Rev. Lett.* **111**, 232302 (2013)
- [7] N. Borghini and J.-Y. Ollitrault, *Phys. Lett. B* **642**, 227 (2006)
- [8] C. Gombeaud and J.-Y. Ollitrault, *Phys. Rev. C* **81**, 014901 (2010)
- [9] L. Bravina, B. H. Buschbeck, G. Eyyubova, and E. Zabrodin, *Phys. Rev. C* **87**, 034901 (2013)
- [10] E. Zabrodin, G. Eyyubova, L. Malinina, and L. Bravina, *Acta Phys. Polon. B* **5**, 349 (2012)
- [11] L. V. Bravina *et al.*, arXiv:1311.0747 [hep-ph] (*Phys. Rev. C*, in press)
- [12] I. P. Lokhtin *et al.*, *Comput. Phys. Commun.* **180**, 779 (2009)
- [13] N. S. Amelin *et al.*, *Phys. Rev. C* **74**, 064901 (2006);  
N. S. Amelin *et al.*, *Phys. Rev. C* **77**, 014903 (2008)
- [14] I. P. Lokhtin and A. M. Snigirev, *Eur. Phys. J. C* **46**, 211 (2006)
- [15] K. Tywoniuk, I. C. Arsene, L. Bravina, A. B. Kaidalov, and E. Zabrodin, *Phys. Lett.* **B657**, 170 (2007)
- [16] L. V. Bravina *et al.*, arXiv:1311.7054 [nucl-th]
- [17] S. Chatrchyan *et al.* (CMS Collab.), *Phys. Rev. C* **87**, 014902 (2013)
- [18] S. Chatrchyan *et al.* (CMS Collab.), arXiv:1310.8651 [nucl-ex]
- [19] B. Abelev *et al.* (ALICE Collab.), *Phys. Lett. B* **719**, 18 (2013)
- [20] R. S. Bhalerao, M. Luzum, and J.-Y. Ollitrault, *Phys. Rev. C* **84**, 034910 (2011)
- [21] J. Jia *et al.* (ATLAS Collab.), *Nucl. Phys. A* **910-911**, 276 (2013)
- [22] R. S. Bhalerao, J.-Y. Ollitrault, and S. Pal, *Phys. Rev. C* **88**, 024909 (2013)